ACS Catalysis

Research Article

pubs.acs.org/acscatalysis

Influence of ZrO_2 Structure and Copper Electronic State on Activity of Cu/ZrO_2 Catalysts in Methanol Synthesis from CO_2

K. Samson,[†] M. Śliwa,[†] R. P. Socha,[†] K. Góra-Marek,[‡] D. Mucha,[†] D. Rutkowska-Zbik,[†] J-F. Paul,[§] M. Ruggiero-Mikołajczyk,[†] R. Grabowski,*[,†] and J. Słoczyński[†]

[†]Jerzy Haber Institute of Catalysis and Surface Chemistry PAS, ul. Niezapominajek 8, Krakow, Poland

[‡]Faculty of Chemistry, Jagiellonian University in Kraków, Ingardena 3, 30-060 Kraków, Poland

[§]University of Lille, Université Lille 1, 59655 - Villeneuve d'Ascq Cedex, France

Supporting Information

ABSTRACT: Cu/ZrO_2 catalysts obtained by impregnation of ZrO_2 and complexation with citric acid were studied for CO_2 hydrogenation to methanol. The catalyst structure, texture, and active copper surface were determined using XRD, BET, and reactive adsorption of N_2O, respectively. The XPS and Auger spectroscopies were used to determine the surface structure and copper electronic state. FT-IR pyridine adsorption was studied to determine acidity of the catalysts. The results of quantum-chemical calculations concerning the formation of oxygen vacancies in monoclinic and tetragonal ZrO_2 have been also presented. It was found that selection of the appropriate conditions of the catalyst preparation influences the degree of copper dispersion, its electronic state, and contents of the zirconia polymorphic phases (tetragonal and monoclinic). The presence of oxygen vacancies stabilizes both the thermodynamically unstable t-ZrO_2 phase and Cu^{1+} cations, which are present in the vicinity of oxygen vacancies. Complexes formed preferentially on tetragonal ZrO_2 built from Cu cations and oxygen vacancies are the acid centers active in methanol synthesis reaction; therefore the catalytic activity toward methanol increases with increasing t-ZrO_2 content. The implications of the obtained results for the mechanism of the catalytic hydrogenation of CO_2 are discussed.

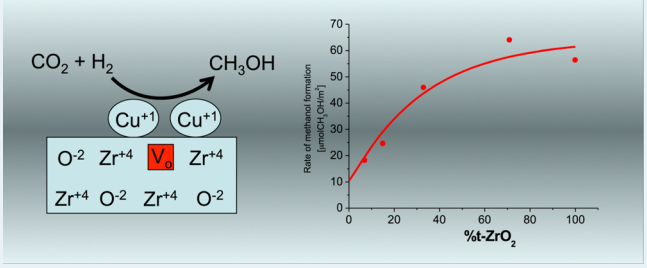

KEYWORDS: *CO_2 hydrogenation, tetragonal and monoclinic ZrO_2, oxygen vacancies, copper zirconia catalysts, methanol synthesis*

1. INTRODUCTION

Methanol is a key material for C1 chemistry[1] and until today has been produced on a large scale from synthesis gas with the use of heterogeneous catalysts.[2,3] Recently, the synthesis of methanol from CO_2/H_2 feedstock has been intensively studied on account of several reasons:

- Utilization of CO_2 waste allows reduction of the greenhouse effect.[4−6]
- Methanol may be a mobile source of hydrogen to supply the cells in the hydrogenation−steam reforming cycle.[7−9] Steam reforming of methanol can be easily performed at the destination, which allows elimination of the inconvenience of hydrogen transportation.
- Methanol is an intermediate product in the dimethylether (DME) formation, considered to be a promising and environmentally benign fuel for diesel engines. Processing of CO_2 originating from renewable sources is a good example of a modern energy source, taking into account environmental protection. Such research is carried out in a number of chemical corporations such as Hader, Topse, Navistar, and Japanese JFE Holding.

It has been well documented that systems containing copper and ZrO_2 in combination with other oxides (e.g., ZnO, Al_2O_3, Cr_2O_3) are active in CO_2 hydrogenation to methanol.[10−25] Despite extensive research on the effects of the copper dispersion and its electronic state on the catalytic activity of these catalysts, the reaction mechanism has not been fully elucidated.

Recently, it was observed that the Cu/ZrO_2 catalytic activity in CO_2 and CO hydrogenation is also dependent on the structure of zirconium oxide. The monoclinic phase of zirconium oxide (m-ZrO_2) is stable at low temperatures, whereas its tetrahedral (t-ZrO_2) phase[26] is stable above 1600 K. The transition temperature is dependent on the defect degree of the crystallographic lattice and the presence of additives. As a result of these effects, the t-ZrO_2 phase appears frequently at low temperatures as a metastable phase. The presence of amorphous ZrO_2 (a-ZrO_2) is also observed at low temperatures.

The results of catalytic measurements on the activity of Cu/ZrO_2 catalysts containing different ZrO_2 polymorphic phases are ambiguous. The results obtained by Baiker et al.,[25] Koppel

Received: July 10, 2014
Revised: September 2, 2014
Published: September 8, 2014

 © 2014 American Chemical Society dx.doi.org/10.1021/cs500979c | ACS Catal. 2014, 4, 3730−3741

et al.[27] and Ma et al.[28] suggest that the presence of t-ZrO_2 promotes the methanol formation from CO and CO_2. A similar result was obtained by Wang et al.[29] for the steam reforming of methanol. However, according to Bell and Jung[30] and Rhodes and Bell,[31] m-ZrO_2 is more active in the methanol formation. The authors assign changes in the catalytic activity to the differences in their acidity. It should be noted, however, that the preparation conditions of both types of ZrO_2 vary considerably. A precursor of the monoclinic phase of ZrO_2 was precipitated in a strongly acidic (pH = 1) environment, while the tetragonal phase was obtained in alkaline solution (pH = 10). In this situation, one would expect the significant difference in the surface hydroxylation and consequently differences in their acidity not related to the support crystallographic structure.

The surface of zirconia offers a variety of active sites. Among them, acidic and basic hydroxyl groups (Brønsted sites) and coordinatively unsaturated Lewis acidic Zr^{4+} cations can be distinguished.[32−36] It has been reported recently[37−39] that all types of sites can contribute to the progress of catalyzed reactions involving CO and CO_2, e.g., the synthesis of branched hydrocarbons from CO/H_2 and the synthesis of methanol from CO/H_2 or CO_2/H_2. The concentration of the structural defects in zirconia, being catalytically active, is generally dependent on the kind of polymorph.[32−36] The Lewis acidic sites, even more abundant on the surface of the monoclinic ZrO_2 phase, were found not to be as strong as those populated on the tetragonal ZrO_2 polymorph.[37,40]

The results of the sorption of CO and CO_2 on the surface of m-ZrO_2 and t-ZrO_2 evidenced the strong dependence between the phase of zirconia and the strength of CO and CO_2 interactions.[37,40] Adsorption of CO_2 on monoclinic ZrO_2 resulted in formation of bicarbonate and monodentate and bidentate carbonates, whereas the principal species observed on t-ZrO_2 were defined as bidentate and polydentate carbonates. Additionally, a significantly higher CO_2 adsorption capacity of m-ZrO_2 than that of tetragonal ZrO_2 polymorph was evidenced. These differences are related to the higher concentration and basicity of the hydroxyl groups as well as the stronger Lewis acidity of Zr^{4+} cations and stronger Lewis basicity of O^{2-} anions in monoclinic ZrO_2 polymorph. Thus, the problem of acidic properties of zirconia support is still wide open for further investigations.

In our recent work[41] on the CO_2 hydrogenation to methanol over Ag/ZrO_2 catalysts, it was shown that the t-ZrO_2 phase is stabilized by the presence of oxygen vacancies and Ag^+ ions incorporated into the zirconia lattice. The methanol formation rate is proportional to the amount of the defected phase. The aim of the present study is to determine whether the regularities observed in the case of the Ag/ZrO_2 catalysts also occur in Cu/ZrO_2 catalysts. Our current research may also help to explain the differences between the results of various authors.

Bulk electronic and geometry structures as well as the morphology of their nanocrystals of both monoclinic and tetragonal ZrO_2 phases were already studied by means of density functional theory (DFT)—see, e.g., refs 42−47. Different morphologies were proposed, based on the relative thermodynamic stabilities of the possible low-index surfaces. Theoretical studies on the influence of the morphology of the zirconia phase on a catalytic reaction are limited only to the water−gas shift process.[48] It is found that both phases differ in the strength of the adsorption process of the products from tetragonal ZrO_2 and the stability of intermediate reactants on the monoclinic ZrO_2.

Model studies on atomic Cu deposited on small cluster of ZrO_2 indicate that Cu activates zirconia by localizing specific nucleophilic and electrophilic reactivity.[49,50] On the basis of DFT calculations and kinetic Monte Carlo simulations, it was proposed that larger agglomerates of copper (strips) on ZrO_2 are located on stepped surfaces, and CO_2 adsorption occurs at the Cu/ZrO_2 interface,[51−53] which is in agreement with experimental findings.[54] The aim of this work is elucidation of the controversy concerning the tetragonal and monoclinic ZrO_2 polymorphs catalytic activity as well as the investigation of the active centers in hydrogenation of CO_2.

The Cu/ZrO_2 catalysts obtained by the method proposed by Bell, i.e., coprecipitation and complexation with citric acid, were examined. In these catalysts, the t-ZrO_2/m-ZrO_2 ratio varies in the range 0−100%. In addition to the catalytic tests, investigations of the crystallographic structure by the XRD method, studies of the catalysts surface structure by XPS and Auger spectroscopies, and the standard acidity measurements using pyridine adsorption were carried out. Quantum chemical calculations concerning oxygen vacancies with the participation of different crystallographic facets in both ZrO_2 polymorphs were carried out.

EXPERIMENTAL SECTION

2.1. Preparation of the Catalysts. The CuO/ZrO_2 precursors were obtained by three, different preparation methods. For synthesis of all samples, Aldrich reagents of 99.99% purity were used. Method 1 involved a coprecipitation process using NaOH (1 M solution) as the precipitant agent. The solution containing appropriate amounts of $Cu(NO_3)_2 \cdot 3H_2O$ and $ZrO(NO_3)_2 \cdot 5H_2O$ and the precipitant solution were added simultaneously, drop by drop, to a beaker containing demineralized water. The precipitation was performed under constant conditions: a temperature of about 353 K, pH of 10, and vigorous mixing at about 350 rpm. After the precipitation, the mother liquid was held at 353 K, under mixing, for 1 h. Then, the mixture was cooled down to ambient temperature, and the precipitate was separated by 5-fold centrifugation at 3500 rpm and washed with demineralized water. Next, the precipitate was dried at 373 K, for 10 h, milled, and subsequently calcinated at 623 K for 5 h, in the flow of air.

Method 2 involved a citric precursor method, using appropriate amounts of 1 M water solutions of metal nitrates (Cu, Zr) and citric acid. Water was evaporated from the solution at 363 K, at pressure achieved with a vacuum pump. The obtained glasslike amorphous product was carried to a heating coat where the citric precursors were decomposed in air at 523 K. Next, the solid sample was dried at 403 K for 8 h and calcined in a stream of air at 623 K for 5 h.

Method 3 described by Bell et al.[30,31] included two separate preparation stages: the synthesis of tetragonal or monoclinic ZrO_2 and then the introduction of the active copper oxide phase on prepared zirconia supports. Tetragonal ZrO_2 was prepared by dropwise addition of 30 wt % ammonia to a 0.5 M solution of $ZrO(NO_3)_2 \cdot 5H_2O$, at a constant pH = 10. The precipitated material was heated in the mother liquid at 373 K, for 20 h, at a pH = 10, under reflux. The obtained product was filtered, washed with H_2O, and dried at 373 K for 24 h. The final thermal treatment consisted of annealing the sample in the flow of air, at 973 K for 5 h. The monoclinic ZrO_2 was synthesized by boiling a 0.5 M solution of $ZrOCl_2 \cdot 8H_2O$ under reflux at 373 K, for 100 h, at a pH = 1.5. The precipitated sample was filtered, washed, and dried in the same way like in

dx.doi.org/10.1021/cs500979c | ACS Catal. 2014, 4, 3730−3741

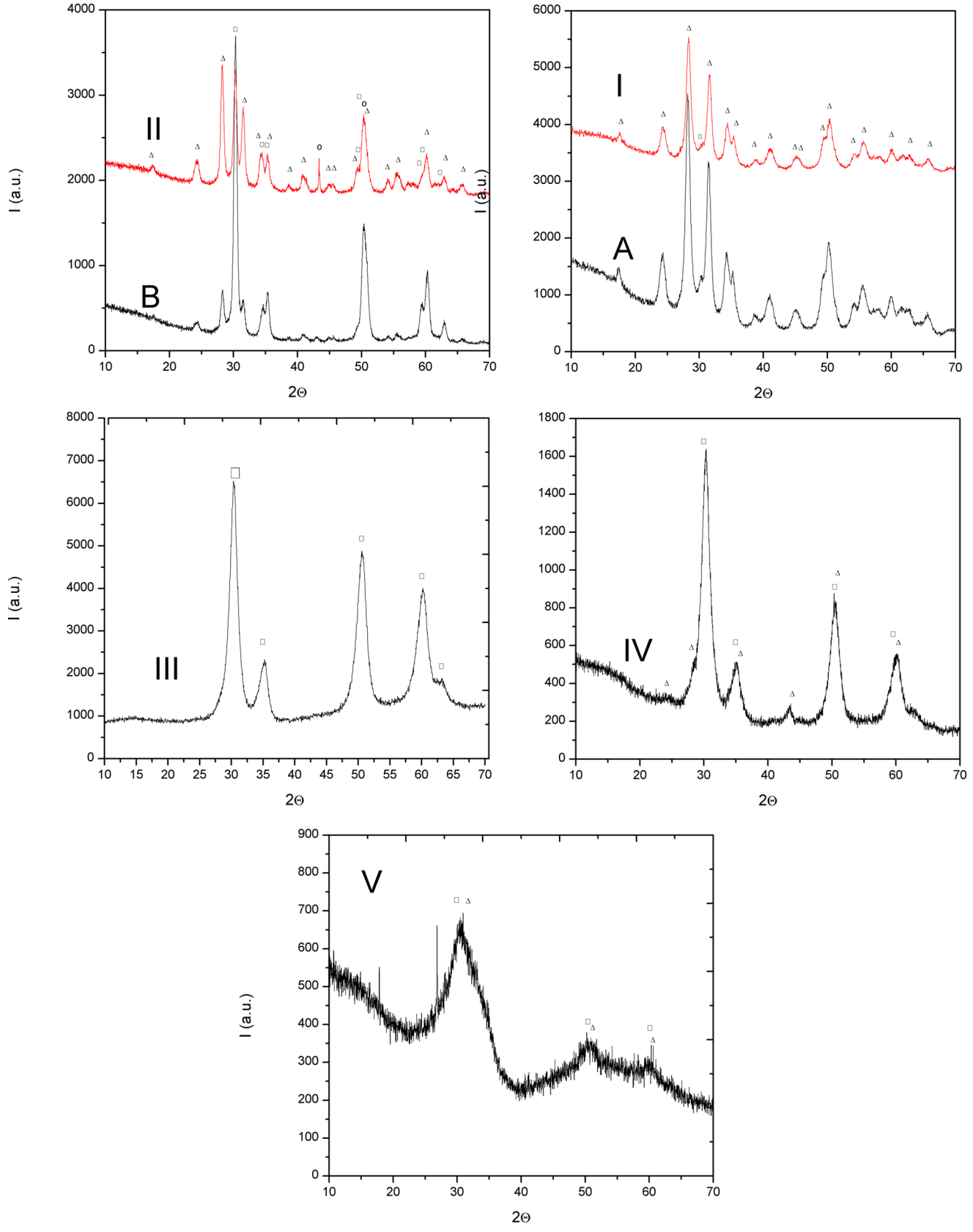

Figure 1. XRD patterns of zirconium carriers (A and B) and catalysts after the methanol synthesis reaction (used catalysts; I to V): Δ, m-ZrO_2; □, t-ZrO_2; ○, Cu.

the case of preparation of the tetragonal zirconia. The final calcination was at 773 K, for 5 h, in a flow of air. The active copper oxide phase was introduced on zirconia supports using the incipient wetness impregnation method, from an aqueous

dx.doi.org/10.1021/cs500979c | ACS Catal. 2014, 4, 3730−3741

solution of $Cu(NO_3)_2 \cdot 3H_2O$. Thus, the received CuO/ZrO_2 samples were dried at 373 K for 10 h and calcinated at 623 K for 5 h, in the flow of air.

The molar ratio of CuO to ZrO_2 was in the range of 0.11−0.18 (10−15% at Cu). The catalyst's composition was determined with the ICP-OES method using a PerkinElmer Optima 2100DV spectrometer.

2.2. Specific Area and Porosity Determination. The specific surface area and pore distributions of the catalysts were determined with the BET and DFT method using an Autosorb-1 Quantachrome apparatus with nitrogen as the adsorbate at 77.5 K.

2.3. Determination of the Active Copper Surface. Active surface copper in the reduced catalysts was determined with the use reactive adsorption of N_2O at 363 K according to a method described elsewhere.[3] The measurements were carried out in a flow quartz microreactor with a length of 18 cm and an internal diameter of 5 mm. The mass of approximately 0.25 g of a catalyst was reduced at 523 K over 3 h and cooled down to 363 K. Then, 100 μL of N_2O pulses were injected until the reaction was completed. The amount of the reacted N_2O was determined using a mass spectrometer (Pfeiffer Vacuum−Prisma Plus). It has been assumed that the reoxidation of the surface occurs according to the equation

$$2Cu_{(s)} + N_2O = Cu_2O_{(s)} + N_2$$

and 1 m^2 of elemental Cu corresponds to 6.1 μmol O_2.

2.4. XRD Measurements. Diffraction patterns of the oxide precursors and the used (after reaction run) catalysts were collected with a Bruker AXS D505 powder diffractometer. Cu Kα radiation and a graphite monochromator of the secondary beam were used. The quantitative phase contents and the crystallite sizes of the catalyst components were estimated with a multiphase Rietveld refinement using the TOPAS software. The fundamental parameter calculations were carried out according to the approach of Cheary and Coelho.[55] The XRD patterns of used catalysts from all studied catalysts (I−V) and supports are shown in Figure 1. The main diffraction maxima characteristic of two phases are located in the theta range of 10−70°: the thermodynamically stable monoclinic modification (m-ZrO_2) and the tetragonal one (t-ZrO_2), which is unstable at ambient temperature. The Rietveld method was used for deconvolution of the diffraction peaks and the content evaluation of both phases.

2.5. Electron Spectroscopy. X-ray photoelectron spectroscopic (XPS) and X-ray Auger Electron spectroscopy (XAES) measurements were performed using a spectrometer equipped with an Al Kα X-ray source (1486.6 eV, 11 kV, 17 mA) and a hemispherical analyzer (R4000, Gammadata Scienta) and a high pressure reactor (Prevac). The spectrometer was calibrated with the use of Au, Cu, and Ag foils according to ISO 15472:2001. The energy resolution of the system, measured as a full width at half-maximum (fwhm) for the Ag $3d_{5/2}$ excitation line, was 1.0 eV.

The powder samples for XPS analysis were prepared as compressed (5 bar) pellets of 7 mm in diameter. The reduction of the sample compounds was performed in the high pressure reactor in pure hydrogen (6.0, Lindegass) at 250 °C for 1 h. The hydrogen pressure was 1.2 bar with a flow of 50 cm^3/min. After reduction, the reactor was evacuated to UHV, and the sample was transferred to the analysis chamber.

The XPS analysis area was about 3 mm^2. The ultrahigh vacuum (3×10^{-10} mbar, UHV) conditions were maintained, and no gas release or change in the sample composition were observed during the measurements. The CasaXPS 2.3.12 program was applied for the XPS spectra analysis. The electron binding energy (BE) scale of all spectra was calibrated for the maximum of C 1s core excitation at 285.0 eV, where carbon adsorbate was taken as an internal standard. In the spectra, the background was approximated by a Shirley profile. The spectra deconvolution into a minimum number of the components was performed by application of the Voigt-type line shapes (70:30 Gaussian/Lorentzian product). The XPS and XAES analysis depths were estimated at 6.8 and 2.2 nm for ZrO_2, 8.3 and 2.8 nm for $Zr(OH)_4$, 3.0 and 1.0 nm for Cu, 3.7 and 1.2 for CuO or Cu_2O, and 4.3 and 1.4 for $Cu(OH)_2$ provided that the bulky form was uniform.[56] The calculations took into account 95% of the overall photoelectron intensity.

2.6. Acidity Measurements. FT-IR pyridine adsorption was used to distinguish the Brønsted and Lewis acidity in studied materials. Prior to the IR studies, each sample of the catalyst (10 mg of catalyst diluted with 20 mg of SiO_2 [POCH]) was outgassed and activated at 570 K, maintained at this temperature for 1 h, and then cooled down to 370 K. The excess of pyridine was adsorbed at 370 K, and physisorbed molecules were subsequently removed by evacuation at the same temperature. The concentration of Brønsted and Lewis acid sites was calculated from the intensities of the 1545 cm^{-1} band for pyridinium ions PyH^+ and of the 1450 cm^{-1} band for pyridine bonded coordinately to Lewis sites, PyL. The values of extinction coefficients were 0.07 and 0.1 μmol/cm^2 for the PyH^+ and PyL bands, respectively.

Sorption of pyridine was preformed also on pure SiO_2 used for dilution of the studied catalysts. No Brønsted acidity was detected for SiO_2. For the CuO/ZrO_2 catalysts, the negligible concentration of Lewis acid sites present in SiO_2 was considered.

The acid strength was determined based on pyridine desorption studies. In the Py experiments, the conservation of the Py bonded to Lewis, Py-L (1445−1452 cm^{-1}), and Brønsted, PyH^+ (1547 cm^{-1}), acid sites band under the desorption procedure at elevated temperature (470 K) has been taken as a measure of the acid strength of the acid sites. The ratio A_{470}/A_{370}, with A_{470} and A_{370} being the intensities of the PyH^+ and Py-L bands recorded after desorption at respectively 470 and 370 K, has been taken as the measure for the acid strength of the protonic and Lewis sites.

2.7. Catalytic Measurements. The activity of the catalysts was tested in the high pressure fixed bed flow stainless steel reactor made by "PID ENG&Tech" (vol. ca. 8 cm^3) connected online to a gas chromatograph (Hewlet_Packard 5800 series II), equipped with a TCD detector (analysis of H_2, CO, and CO_2) and a FID detector (organic compounds). All lines were heated to 393 K to prevent condensation of methanol and water. The reactor internal diameter was 8 mm; a thermocouple was placed in the middle of the catalyst layer, which was placed between two layers of porcelain of the same grain size as the catalyst. A total of 1 cm^3 of catalyst with a grain size 0.64−1 mm was placed into the reactor. The oxide precursors were reduced in a stream of diluted hydrogen (5 vol % H_2 in N_2) at 473 K for 3 h under atmospheric pressure and activated in the mixture of reactants by raising the temperature by steps of 30° between 473 and 623 K every 2 h. The catalytic activity in the methanol synthesis was determined under the following conditions: a pressure of 8 MPa, temperature range of 453−533 K, space velocity of the reactants flow of GHSV = 3600

dx.doi.org/10.1021/cs500979c | ACS Catal. 2014, 4, 3730−3741

Table 1. Characterization of the Studied Catalysts

catalyst	preparation method	surface area [m^2/g] before/after reaction	pore volume [cm^3/g]	average pore diameter [nm]	t-ZrO_2 content [%]	ZrO_2 mean crystal size [nm]	Cu surface area [m^2/g_{cat}]	Cu dispersion [%]	number of Cu monolayers
				supports					
ZrO_2 (A)	according to bell calcined at 773 K	57.2/-			9	14.5			
ZrO_2 (B)	according to bell calcined at 973 K	50.6/-			60	26.5			
				catalysts atom % of Cu					
Cu/ZrO_2 (I) 15	impregnation of ZrO_2(A), calc. at 623 K	50.4/47.8	0.09	7	7	9.4	2.11	4	1.87
Cu/ZrO_2 (II) 10	impregnation of ZrO_2(B), calcd. at 623 K	45/43.6	0.24	21	33	23.7	5.58	16	1.34
Cu/ZrO_2 (III) 10	complexation with citric acid, calcd. at 623 K	101/61.9			71	6.5	2.77	8	0.94
Cu/ZrO_2 (IV) 10	complexation with citric acid, calcd. at 773 K	85.5/47.7	0.05	4	100	7.1	1.73	5	1.22
Cu/ZrO_2 (V) 10	precipitation with NaOH, calcd. at 623	182/128.5			15	3.9	1.49	4	0.45

h^{-1}, and composition of the reactant mixture H_2/CO_2 = 3. It was checked in the preliminary experiments, in which mass and grain size of the catalysts were varied and the temperature profile was determined, that under these conditions mass and heat transfer did not limit the reaction rate. After the reduction and activation, the catalysts showed a constant activity for 10 days in the cycles of the temperature increase and decrease. After the tests, the catalysts were cooled down to room temperature in the reaction mixture. Such catalysts are named in this paper "used catalysts." It is assumed that the composition and structure of the used catalysts correspond closely to the composition and structure of the working catalysts at the stationary state, which is established under conditions of the catalytic reaction.

2.8. Methodology of Quantum Chemical Calculations. Oxygen vacancy formation on different tetragonal and monoclinic ZrO_2 surfaces was modeled assuming that oxygen is removed as a water molecule; thus the energy of vacancy formation was computed as

$$E_{vac} = E(ZrO_2, vac) + E(H_2O) - E(ZrO_2) - 2E(H)$$

The reported calculations were performed with the VASP code[57,58] using the PW91 functional.[59,60] Electrons are described by PAW[61,62] with a default cutoff energy of 450 eV with 5 × 5 × 1 k-point sampling mesh. A detailed description of the computational procedure is given elsewhere.[42,43]

3. RESULTS

3.1. Phase Composition and Morphology of the Catalysts. XRD diffraction patterns of zirconium carriers and catalysts after the methanol synthesis reaction (used catalysts) are shown in Figure 1. The Rietveld method was used for diffraction peak deconvolution and the content evaluation of both phases, i.e., tetragonal and monoclinic. As can be seen in the case of the catalyst prepared by coprecipitation of (Cu/ZrO_2−V), only microcrystalline zirconium oxide is present, as evidenced by the diffraction pattern in the range of 10° to 70° (2 theta). In the case of the remaining catalysts, diffraction maxima characteristics for both phases of zirconium oxide are sharp and well-separated. Only in the catalyst prepared by impregnation of the carrier, which is enriched in t-ZrO_2 (Cu/ZrO_2 II), are Cu crystallites observed. In other catalysts, copper is present in the highly dispersed or amorphous form. XRD results of the quantitative analysis obtained by the Rietveld method are shown in Table 1. It also contains data on the surface area of the catalysts, Cu dispersion, and active copper surface.

Determination of the pore distribution showed that all studied catalysts are mesoporous. Almost all the studied catalysts have the same copper content (∼10 atom % Cu). Only in the case of catalyst I, in which m-ZrO_2 was prevailing, was 15 atom % Cu introduced because of low catalytic activity. The nominal copper coverage calculated using 14.4 μmol Cu/m^2, taken from ref 63, are in the range 0.5 to 1.8 monolayers number.

The data in Table 1 indicate that the oxide precursors change their properties as a result of their reduction and prolonged time of contact with the reactant mixture. The most dinstinctive changes concern the surface area of the catalysts in which microcrystalline ZrO_2 is present, i.e., the catalysts obtained by citrate and the coprecipitation method. The catalysts prepared by impregnation of the zirconia support calcined at relatively high temperatures are more stable. Nevertheless, even in this case, one can see the changes in the surface area, which correlate with the increase of ZrO_2 crystallite size, and also the changes in the concentration of different polymorphs are also observed. The results described above indicate that, during the catalytic reaction, the processes of copper oxide reduction and sintering of the catalyst components take place. Therefore, redistribution of Cu especially in the subsurface area should be expected.

The size of the active surface of metallic copper (Table 1) of the used catalysts varies slightly; only the Cu/ZrO_2 II catalyst, prepared by zirconia impregnation, which was calcined at a relatively high temperature (973 K), is characterized by a significantly higher value of the Cu active surface. This result corresponds to the presence of Cu crystallites, confirmed by the XRD method. In the studied catalysts, the surfaces of the active copper, recalculated to 1 g of Cu, are within the limits of 25−

dx.doi.org/10.1021/cs500979c | ACS Catal. 2014, 4, 3730−3741

Table 2. Catalyst Surface Quantitative Analysis of the Electronic State of Copper Obtained on the Basis of XPS Results[a]

			Cu/Zr			Zr/O*			Cu^0	Cu^{+1} Cu^{+2}	OH
catalyst	Cu/Zr nominal	wt % t-ZrO_2	F	U	UH_2	F	U	UH_2		UH_2	
I	0.18	7	0.18	0.22	0.28	0.58	0.57	0.59	79	4	17
II	0.10	33		0.13	0.12		0.60	0.60	62	25	13
IV	0.10	100		0.09	0.07		0.63	0.63	10	80	10

[a]O* lattice oxygen (after subtraction water oxygen). F, fresh catalyst; U, used catalysts; UH_2, used catalyst reduced *in situ*.

100 m^2, which is typical for Cu/ZrO_2 catalysts with a low copper content.

Despite applying preparation conditions used by Bell et al.,[30] one failed to obtain pure polymorphic zirconium oxide phases (monoclinic and tetragonal). This methodology is quite complicated, and perhaps an important role is played by the factors not included in the description of the procedure. In our work, we have shown, however, that using a simple method of complexation with citric acid, the catalysts containing pure t-ZrO_2 phase can be obtained. The series of catalysts (I–V; Table 1), in which the content of THE tetragonal phase varies from close to zero to 100%, was obtained by different preparation methods.

3.2. Surface Properties of the Catalysts. The samples were investigated by XPS and XAES. Among the catalysts described in Table 1, three catalysts were chosen, which differ with the preparation method and the content of polymorphs of ZrO_2. These are catalyst I obtained by impregnation of ZrO_2 support, containing mainly the monoclinic phase, catalyst II obtained by the same method containing 33% of t-ZrO_2, and catalyst IV obtained by complexing with citric acid, which contained 100% t-ZrO_2. The analyzed catalysts (used) were at first reduced and activated in the feed mixture and then worked-out in a reactor for several hours in the temperature range of 473–533 K. Since it was found that copper in these catalysts oxidizes in contact with air, even at room temperature, the used catalysts, which were reduced in situ by hydrogen before the spectroscopic measurements in order to restore their electron state before reoxidation, were also tested. Further on, in this text, the most representative results are described, and whole experimental material is collected in the SI (Supporting Information).

The O 1s core excitation envelope, for all studied samples, was deconvoluted (Figures 1–3, SI) into three components assigned to oxygen in the metal oxide lattice (O_A, component A), oxygen in hydroxyl groups (B, O_B), and oxygen in adsorbed water or organic compounds (C, O_C).[64−66] In most analyzed surfaces, the oxide lattice oxygen at BE of approximately 530 eV was found as the predominant species. The surface of catalyst I after methanol synthesis shows a larger amount of OH groups (40.0%) than observed for the citric (IV) type catalyst (31.7%). The ability to form hydroxide species at the catalyst surface during methanol synthesis confirms lower stability of the catalyst surface in the case of Bell type synthesis than in the citric one.

The Zr 3d core excitations were deconvoluted (Table 1SI, Figure 1–3SI) into two doublets assigned to Zr^{4+} in the ZrO_2 lattice (component A) and Zr^{4+} in strongly electrophilic surroundings like bonding to OH groups (B).[64−67] The surfaces of the citric (IV) type catalysts after methanol synthesis or hydrogen reduction showed limited changes suggesting high stability of the zirconia lattice. The zirconia structure obtained in the synthesis of catalyst I revealed higher ability for the Zr^{4+} ion hydroxylation (Figure 1–3SI). Catalyst I, when reduced in hydrogen, showed a higher amount of hydroxyl bonded zirconium ions than catalyst IV obtained by the citric method, where the opposite tendency was observed (Table 1SI).

The Cu/Zr atomic ratios determined from XPS measurements (Table 2) were close to the nominal values wherein the impregnated catalysts' surface layer was enriched in Cu.

In the catalysts obtained by complexing with citric acid, the determined copper concentration was a little lower in respect to nominal content. The $Zr/(O_{(A)}+O_{(B)})$ ratio for studied catalysts was always higher than 0.5, which suggested oxygen deficiency in the ZrO_2 lattice, i.e., the presence of oxygen vacancies. The highest concentration of vacancies was observed in the catalyst, which contained only the tetragonal phase of ZrO_2.

As an example, the Cu 2p XPS and Auger spectra of catalyst II after the CO_2 hydrogenation reaction and their reduction by hydrogen are presented in Figure 2. They were deconvoluted into three components: A (assigned to Cu^{1+}), B (metallic Cu), and C (Cu^{2+} OH) (Table 1SI). For all unreduced catalysts, the intensity ratio of shakeup satellites to respective photoelectron

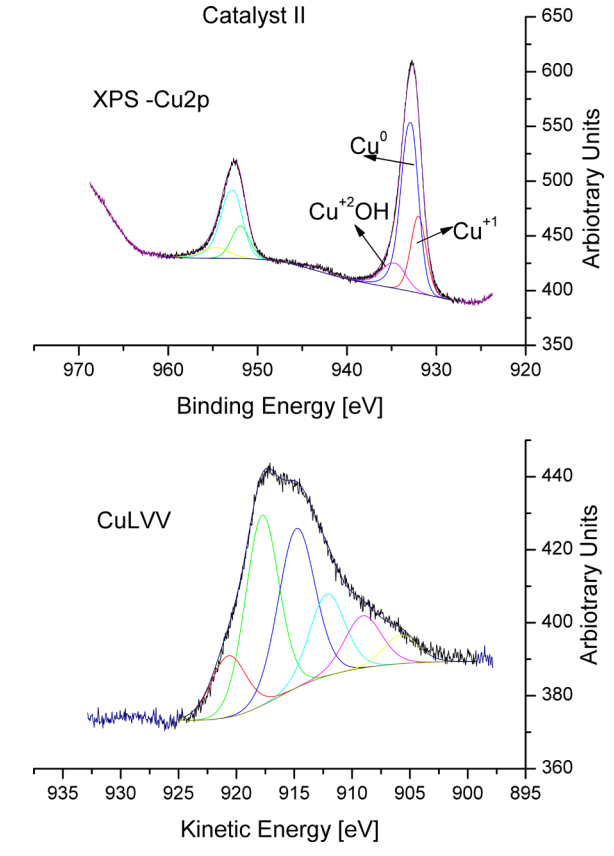

Figure 2. Example of Cu XPS and Auger Cu LVV excitation spectrum for catalyst II after reaction and hydrogen reduction.

dx.doi.org/10.1021/cs500979c | *ACS Catal.* 2014, 4, 3730–3741

peaks suggested a significant contribution of Cu^{2+} ions in the surface composition. Additionally, the XAES spectra helped to calculate the modified Auger parameter (α'; Table 2SI), which, when valued on the so-called Wagner plot,[65] can determine the electronic state of copper much more precisely. Thus, the Cu 2p spectra showed that Cu^{2+} in an oxide lattice is the main component of unreduced catalyst samples.[56,64−68]

In the case of hydrogen reduced catalysts (Table 3), the BE of Cu $2p_{3/2}$ suggests that the main surface species can be metallic copper and/or Cu^+ in an oxide lattice.[64−67,69]

Table 3. Electronic State of Copper for Used Catalysts Reduced *in Situ* Obtained on the Basis of Auger Results

catalyst	BE Cu $2p_{3/2}$ [eV]	KECuL_3 VV [eV]	α'[eV]	assigment	Cu^+/Cu^{2+}
I	932.6	918.6	1851.2	Cu^0	1.48
II	932.7	917.8	1850.5	Cu^0	1.09
IV	932.4	918.6	1851.0	Cu^0	1.05

The above conclusion is supported by the Auger parameter values, which approached 1851.0 eV, indicating metallic copper at the surface (Table 3). In a similar way, for the catalysts after methanol synthesis, α' suggests the presence of Cu^{2+} ions in surroundings much different from the CuO lattice. The relatively low value of KE at a maximum of Cu L_3VV excitation indicated that Cu^{2+} ions, in this case, should be located in strongly electronegative surroundings, such as that observed in zeolites.[68−70] This can suggest any interaction of the Cu ions with the zirconia support.

For the used catalysts reduced in situ, the data concerning the content of the particular copper species on different oxidation states are given in the last column of Table 2. These results indicate that the increase of the t-ZrO_2 content in Cu/ZrO_2 catalysts leads to a decrease of the amount of metallic copper and an increase in content of the Cu^+ cationic form, whereas the content of Cu^{2+} changes slightly.

It is worth noticing that analysis of copper compounds must be supported by both the XPS and XAES methods. The XPS signal acquires information from about 10 monolayers and XAES from about 3. Additionally, an analysis of the shape of Cu L_3VV spectra (Figure 2SI) before and after reduction in hydrogen showed that a component at KE at about 915 eV was present in the Cu LVV spectrum also after the catalyst reduction in hydrogen. That KE value can be assigned to either Cu^{2+}[67,70] or Cu^+.[67,71] An analysis of the Cu L_3VV spectra of model systems of CuO/ZrO_2 and Cu_2O/ZrO_2 from Espinos et al.'s work[67,69] allowed the conclusion that both Cu^{2+} and Cu^+ ions are present in the analyzed samples where Cu^{2+} is predominant. The approximation of the Cu^+/Cu^{2+} ratio can be performed by comparison of Cu L_3VV components at a KE of approximately 918 eV, a maximum for all reduced samples, to a component at about 915.5 eV, ascribed to Cu^{2+} ions. These results are collected in Table 3. The approximation indicates that all reduced samples showed a ratio above 1, whereas for unreduced ones, the ratio was below 1. Thus, it can be again stated that the catalyst obtained by complexation with citric acid (IV) showed a lower ability (lower amount of Cu^+ species) to be reduced when compared to catalyst I.

Therefore, the hydrogen reduced surface of the copper active sites can be modeled as covered by metallic copper at the top, whereas Cu^{2+} and Cu^+ ions are located underneath with the ratio depending on catalyst type. In the case of the surface modified in methanol synthesis, the outermost part can be composed of Cu^{2+} ions dispersed in zirconia lattice. The surface of a fresh catalyst I obtained by the Bell method shows Cu^{2+} in the form of CuO, confirmed by both electron spectroscopies. In summary, the analysis of a variety of copper species and their amount at the IV and Bell type catalysts suggests a higher ability of I catalyst to be modified in a much more complicated manner than in the case of IV catalyst. This surface modification is observed in both hydrogen reduction and methanol synthesis.

3.3. Acidity of the Catalysts. Figure 3 depicts the spectra of pyridine adsorbed on studied samples allowing the distinction of the Brønsted and Lewis acidity. The Brønsted acid sites are revealed only in the ZrO_2 tetragonal polymorph, as shown by the PyH^+ band at 1547 cm^{-1}, while the Lewis acid sites are present in both polymorphs. However, the bands of PyL are observed on both monoclinic and tetragonal zirconia; they appear at different frequencies. For monoclinic ZrO_2 (spectrum a), the bands of pyridine bonded coordinatively to the Lewis sites appearing at lower frequencies (1445 cm^{-1}) than for tetragonal polymorph catalysts (the band of Py-L at 1452 cm^{-1}; spectrum b). This observation refers to higher thermal stability of Lewis sites on the surface of t-ZrO_2, indicating that the Lewis acidity of Zr^{4+} cations is higher for tetragonal surfaces. The same conclusions can be drawn from the analysis of the results of the pyridine thermodesorption collected in Table 4.

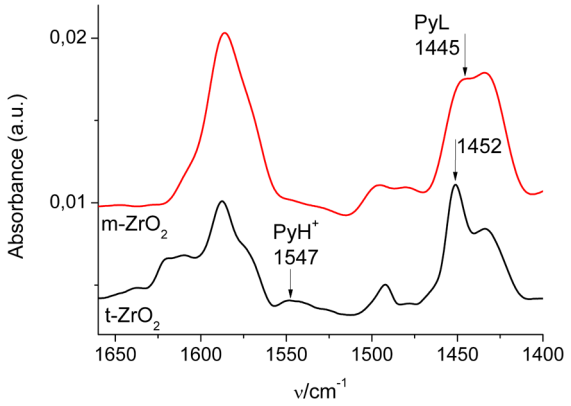

Figure 3. IR spectra of pyridine adsorbed on A and B ZrO_2.

Table 4 summarizes the results of the quantitative pyridine sorption experiments for pure supports (m- and t-ZrO_2) and samples modified with CuO. Despite the fact that both polymorphs revealed the same concentration of Lewis acid

Table 4. Brønsted (BAS) and Lewis (LAS) Acidity of the Studied Catalysts

catalyst	BAS [μmol/m^2]	LAS [μmol/m^2]	strength of BAS	strength of LAS
ZrO_2(A)	0/0.17*	0.87	-/0	0.20
ZrO_2(B)	0.40	0.89	0	0.40
Cu/ZrO_2 (I)	0.52	3.14	0	0.30
Cu/ZrO_2(II)	0.73	4.13	0.15	0.55
Cu/ZrO_2(III)	0.89	4.94	0.13	0.75
Cu/ZrO_2(IV)	0.94	4.72	0.30	0.60
Cu/ZrO_2(V)	0.40	0.93	0.10	0.35

dx.doi.org/10.1021/cs500979c | ACS Catal. 2014, 4, 3730−3741

sites, in t-ZrO_2, the acid sites are of significantly higher strength (A_{470}/A_{370} = 0.20 for m-ZrO_2 vs 0.40 for t-ZrO_2). Additionally, the concentration of electron acceptor sites is at least 2-fold higher than the protonic ones.

Deposition of CuO on ZrO_2 supports resulted in the appearance of some amount of Brønsted acid sites. This kind of species can be formed on the surface of CuO/ZrO_2 due to its ability to adsorb and then dissociate water on highly stable oxygen vacancy defects.[39,72] An enhanced Brønsted acidity has also been reported for CuO_x/WO_x–ZrO_2 catalysts.[73] In addition, a significant increase of the Lewis acid site concentration is detected at ZrO_2 as a result of the copper ions' presence. The strength of newly created Lewis sites was also found to be higher than for the nonmodified support, suggesting their high electron acceptor properties. Similarly to m-ZrO_2, the presence of CuO on tetragonal ZrO_2 results in the enhancement of the number of both Brønsted and Lewis acid sites. Nevertheless, the increase of the Lewis acid sites contribution to global acidity is 4–5-fold higher when comparing to the pure t-ZrO_2 support. The Lewis acid sites of considerably high strength are found also for CuO/t-ZrO_2. The influence of CuO introduction on the enhanced acid properties of ZrO_2 catalysts can suggest the strong interaction between copper and zirconia ions. It was reported that the catalytic activity increased with the strength of interaction between CuO and ZrO_2.[74] As a p-type semiconductor, the work function of ZrO_2 is higher than that of copper; thus the strong interaction between CuO and ZrO_2 results in electron deficiency on copper. Consequently, due to the presence of stronger interaction between copper species and ZrO_2, the Zr species have been evidenced to lead to the facile reduction of Cu^{2+} to Cu^{+}/Cu^{0}.[73,74] Strong interactions between the highly dispersed active CuO component and the tetragonal ZrO_2 support resulted in the presence of Lewis acidic sites of both high strength and high abundance. Such species are supposed to be responsible for the higher CO_2 conversion and high methanol yield.

3.4. Stabilization of Tetragonal ZrO_2 in Cu/ZrO_2 Catalysts. Table 5 collects computed oxygen vacancies' formation energies on different facets of both tetragonal and monoclinic ZrO_2, their relative abundances (taken from refs 42 and 43) at temperatures not exceeding 550 K, which are relevant to the experimental conditions, and mean oxygen vacancy formation in the crystal of each phase computed upon these data, according to the formula

$$E_V = \sum_n E_{VAC}(\text{surf } n) \times \text{cont}(\text{surf } n)$$

where E_{VAC}(surf n) is the energy of vacancy formation on surface n and cont(surf n) is the abundance of surface n at a given temperature.

It is found that it is easier to create vacancies in the tetragonal phase than in a monoclinic one in the studied temperature range. This result is a consequence of the fact that participation of (111) facets, on which the oxygen vacancies are formed much easier, is higher in t-ZrO_2 in comparison with the monoclinic polymorph.

The importance of oxygen ion vacancies in ZrO_2 was suggested by different research groups.[75] Such oxygen vacancies are generated either at higher temperature or due to doping with different impurities. There are several reports in the literature which support the hypothesis that the tetragonal phase in doped ZrO_2 is stabilized at a higher temperature

Table 5. Computed Energies of Oxygen Vacancy Formation on Different Surfaces of Monoclinic and Tetragonal Zirconia and Mean Energies of Oxygen Vacancy Formation on ZrO_2 Nanocrystallites

		relative abundances of different facets[a] (% content)		
tetragonal	E_{vac} [eV]	T = 0 °C	150 °C	300 °C
101	3.77	6	12	35
001	4.42	8	12	11
100	3.12	8	13	13
111	2.25	49	48	26
110	2.70	28	15	15
E_{vac}^{mean} [eV]		2.69	2.87	3.20
		(% content)		
monoclinic	E_{vac} [eV]	T = 0 °C	150 °C	300 °C
−111	3.31	45	24	20
111	2.25	24	21	22
011	2.90	6	38	45.5
001	3.57	16	11	12
101	2.29	0	3	0.5
100	3.28	10	3	0
E_{vac}^{mean} [eV]		3.43	3.24	3.22

[a]Relative abundances of different surfaces are taken from refs 42 and 43.

because of the oxygen vacancies' presence.[76−78] In addition, the presence of various anions such as OH^{-}[79] and CO_2^{-}[80] within the ZrO_2 lattice stabilizes the tetragonal phase at room temperature.

As found by Dviwedi and Cormack,[81] the dopant atoms such as Ca are coordinated by a full complement of oxygen atoms, and the formal anion vacancies are nearest neighbors to Zr atoms. However, in another paper,[82] it was found that the anion vacancies tend to be rather nearest neighbors to the dopant atoms than Zr. This finding is also supported by results obtained in ref 83, where authors showed that charge excess of divalent impurities in zirconia is compensated by oxygen vacancies, and at high temperatures, in dipoles the impurity–vacancy is very closely located relative to each other and anion vacancies are mobile. Both cation impurities and oxygen vacancies can be considered as randomly distributed among lattice sites and can occupy the nearest-neighbor or next-nearest-neighbor sites.

According to Stefanovich and Shluger,[83] the main factors, which have influence on the stabilization mechanism of the cubic and tetragonal zirconia phase by impurities, are the lattice distortion around vacancies, lowering of the dielectric constant, and increasing of the zirconia ionicity by the addition of divalent impurities.

3.5. Catalytic Activity of the Catalysts. Methanol, water, and carbon monoxide were the only products of CO_2 hydrogenation under the conditions of the catalytic tests. The results of the catalytic tests are collected in Table 6.

It was generally accepted that the reaction occurs according to the following parallel reactions:[2,3]

$$CO_2 + 3H_2 \leftrightarrow CH_3OH + H_2O \quad (1)$$

$$CO_2 + H_2 \leftrightarrow CO + H_2O \quad (2)$$

In our experiments, the total conversion of CO_2 was between 0 and 15%, depending on the temperature and activity of the catalysts, but generally conversion was low, so the hydro-

dx.doi.org/10.1021/cs500979c | ACS Catal. 2014, 4, 3730−3741

Table 6. Catalytic Activity of the Cu/ZrO_2 Catalysts in CO_2 Hydrogenation to Methanol

catalyst	temperature [K]	CO_2 conversion [%]	selectivity [%] methanol	selectivity [%] CO	methanol formation rate [μmol CH_3OH/(m^2 h)]
ZrO_2	473	0	0	0	
	493	0	0	0	
	513	0	0	0	
	533	0.5	100	0	
Cu/ZrO_2(I)	473	0	0	0	
	493	0	0	0	
	513	2.2	100	0	12.8
	533	3.3	100	0	14.1
Cu/ZrO_2(II)	473	1.5	100	0	12.9
	493	2.4	100	0	20.7
	513	3.5	100	0	30.2
	533	5.5	100	0	47.3
Cu/ZrO_2(III)	473	5.3	100	0	26.1
	493	7.8	100	0	38.6
	513	10.7	97	3	53.5
	533	15.0	86	14	63.9
Cu/ZrO_2(IV)	473	2.4	100	0	16.9
	493	3.6	100	0	25.7
	513	5.8	100	0	41.0
	533	8.6	92	8	56.3
Cu/ZrO_2(V)	473	2.4	100	0	6.8
	493	6.4	95	5	17.3
	513	10.5	69	31	20.5
	533	14.0	62	38	24.5

genation of CO_2 to methanol was the main route of the reaction because it was faster than the conversion of CO_2 to CO.[3] The investigated system is far from the equilibrium in such conditions and the reaction is controlled kinetically. The selectivity to methanol decreases with increasing temperature, which is due to a higher contribution of the endothermic RWGS reaction. Tests with both ZrO_2 polymorphs revealed that the zirconia support is inactive in the investigated temperature range. The methanol formation rate referred to the unit of the catalyst surface used for comparison of the activities of Cu/ZrO_2 catalysts. Figure 4 shows the dependence of the methanol formation rate as a function of the content

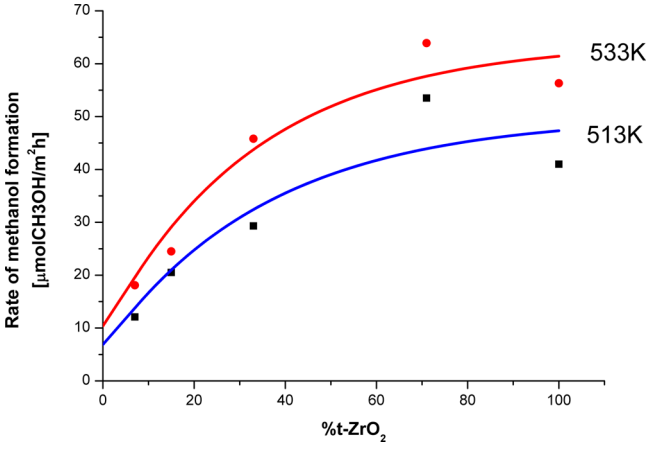

Figure 4. Methanol formation rate as a function of t-ZrO_2 content.

tetragonal polymorph of ZrO_2 in the catalyst. One can see that the catalytic activity increases with increasing content of tetragonal ZrO_2 in the catalyst, which indicates that the $Cu/t\text{-}ZrO_2$ catalyst is a more active component than $Cu/m\text{-}ZrO_2$. At the same time, from Figure 5, Cu/ZrO_2 catalyst activity is

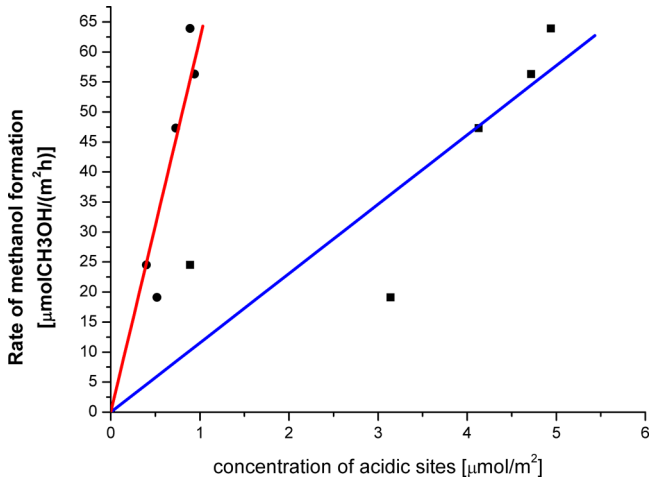

Figure 5. Methanol formation rate at 533 K as a function of the concentration of acidic sites. (■) Lewis acid centers, (●) Brønsted acid centers.

linearly correlated with both forms of acidity (Brønsted and Lewis). Thus, $t\text{-}ZrO_2$ favors the formation of acid sites generating activity of a catalyst in the synthesis of methanol over Cu/ZrO_2. On the other hand, according to data from Table 1 and Table 6, catalytic activity is not correlated with metallic copper dispersion. The average value of methanol formation rate per one acidic center (TOF) for 533 K for Lewis and Brønsted is equal to 3.2×10^{-3} (CH_3OH molecules/s) and 17.3×10^{-3} (CH_3OH molecules/s) respectively. These values are comparable with the TOF values for industrial catalysts $(3.5/10) \times 10^{-3}$ (CH_3OH molecules/s).[3]

4. DISCUSSION

We will begin the discussion by summarizing the existing findings concerning the catalytic activity of ZrO_2 polymorphs. The results of the measurements of the methanol formation rate from CO_2 or CO related to the unit of the catalyst surface obtained by different authors are collected in Table 7.

Since the rate measurements were carried out at different pressures of the reactant mixtures, for comparison, the reaction rate (r) was recalculated for the same value of pressure (8 MPa), using the empirical formula ($r \sim p^{0.65}$).[24]

Figure 6 shows the results obtained in this work (solid lines) in comparison to the reference data in the form of the linear system corresponding to the Arrhenius equation. As can be observed, our results, which show that $Cu/t\text{-}ZrO_2$ is more active in the methanol synthesis from H_2/CO_2 than the $Cu/m\text{-}ZrO_2$ catalyst, correspond to the findings of most authors. It is clearly shown in ref 28, where comparison of the activities of the monoclinic and tetrahedral ZrO_2 polymorphs, as well as amorphous ZrO_2 were carried out. The opposite trend presented by Bell et al.[31] is definitely unique. Furthermore, the reaction rates, determined by these authors for catalysts comprising $t\text{-}ZrO_2$, are very low and significantly differ from the rest of the results. It appears that in the case of a sample of this

dx.doi.org/10.1021/cs500979c | ACS Catal. 2014, 4, 3730−3741

Table 7. Literature Data for Different CuO/ZrO_2 Catalysts Studied in CO_2 Hydrogenation to Methanol

catalyst				methanol formation rate (r^a) [μmol CH_3OH/ (m^2_{cat} h)]					
Cu [atom %]	preparation method	phase composition	specific surface area [m^2/g]	493 K	513 K	533 K	548 K	573 K	references
9	coprecipitation				H_2/CO_2 = 3; 1.7 MPav				25
	calc. 723 K	100% t-ZrO_2	158		11				
	calc. 623 K	100% t-ZrO_2	213		10		14		
50	sequential precipitation	amorphous or microcrystlline	161		H_2/CO_2 = 3; 1.7 MPa				14
				19					
13	low temperature supercritical drying	t≫m	139		H_2/CO_2 = 3; 1.7 MPa				27
					19		20		
	impregnation of supports				H_2/CO_2 = 3; 0.65 MPa 548 K conversion of CO_2/g cat.				30
7	pH < 1	100% m-ZrO_2					1.6[b]		
7	t-ZrO_2 pH = 10	100% t-ZrO_2					6.8[b]		
	deposition precipitatiopn				CO hydrog. H_2/CO = 3; 3 MPa				31
1.1	m-ZrO_2	100% m-ZrO_2	143		20				
1.1	t-ZrO_2	100% t-ZrO_2	150		2				
9	impregnation of ZrO_2 supports calcd. 623 K				CO hydrog. H_2/CO = 2; 2.8 MPa				28
		amorph	148					18	
		100% m-ZrO_2	38					44	
		100% t-ZrO_2	24.5					216	

[a]Rate of reaction (r) recalculated to p = 8 MPa according to formula $r \sim p^{0.65}$ [ref 24]. [b]CO_2 conversion at 548 K

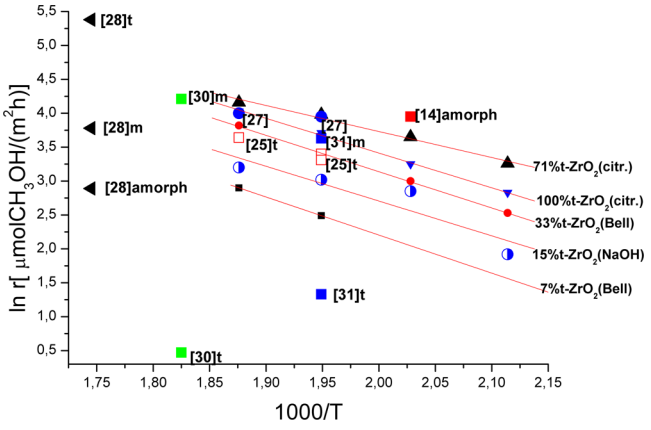

Figure 6. Logarithms of methanol rate formation as a function of $1/T$ obtained on the basis of literature data and our results. Rate of reaction (r) recalculated to p = 8 MPa according to formula $r \sim (0.65)$.[24] References numbers are in square brackets.

catalyst, an additional factor has caused the abnormal decrease in its activity.

The results obtained in this work fully correspond with our earlier findings on the catalytic activity of the Ag/ZrO_2 system.[41] In this work, we have found that the methanol formation rate increases with increasing t-ZrO_2 content phase in the catalyst, and the active centers are Ag^+ ions incorporated into the ZrO_2 network near oxygen vacancies. Action mechanism of the Ag/ZrO_2 and Cu/ZrO_2 catalysts is therefore analogous, but establishing that it is valid for the Cu/ZrO_2 system is more important because this system has high activity and therefore is the component of many active methanol synthesis catalysts used in industrial practice.

The presented studies showed that there is a linear correlation between catalytic activity and acidity of the catalysts for both Brønsted and Lewis centers. This means that in the catalysts with increasing t-ZrO_2 phase content, in parallel with an increase of the catalytic activity, the catalyst acidity increases. Thus, the IR analysis shows that the tetragonal phase stimulates catalyst acidity, which again is in contrast to the findings of Bell et al.[30,31] However, Bell believes that the acidic centers exist only on the surface of ZrO_2 and copper works as an active center for methanol formation only exclusively in metallic form, causing the dissociative adsorption of hydrogen. However, our results show that the acidity of zirconia and its catalytic activity is negligible, while the acidic centers, which are involved in the reaction, are formed with the participation of copper. It is evident that copper present in the centers must be in cationic (Cu^+ or Cu^{2+}) form. At the same time, the results presented in Table 4 show that the concentration of Lewis acid sites is several times higher than the concentration of Brønsted centers, suggesting that the former are responsible for the increase in catalytic activity.

The fact that in our study we found no linear correlation between the methanol formation rate and the surface of metallic copper, which is often observed by other authors, requires comment. Already Joyner[84] noted that the correlation coefficient in this relation in many times is low, which indicates that the active surface of Cu is not the only factor determining the catalytic activity. Burch et al.,[85] Robinson and Mol,[86] and Baiker and Köppel[10] found that the present correlation is not general and is valid rather for a specific series of catalysts in which only one parameter is changed (e.g., Cu loading). Catalysts tested by us were obtained by different methods, resulting in changes of the composition of the zirconia carrier phase by changing the ratio of two polymorphs of ZrO_2 (monoclinic and tetragonal). In this situation, as we have seen, a decisive factor for the rate of formation of methanol proved to be the concentration of acidic centers consisting of Cu cations connected to oxygen vacancy.

Spectroscopic studies (Auger and XPS) showed that at the surface of the catalyst, even after prolonged contact with a mixture of reactants, copper is present not only in metallic Cu^0 form but also as a Cu^+ cation and as the surface copper hydroxide. The concentration of the cationic forms on the substrate depends on the nature of zirconia and is several times

dx.doi.org/10.1021/cs500979c | ACS Catal. 2014, 4, 3730−3741

higher for tetragonal ZrO_2 phase in comparison to monoclinic ZrO_2. Copper ions, which are the components in pure oxides (CuO, Cu_2O) are thermodynamically unstable in a reducing atmosphere but are stabilized by introduction into the ZrO_2 lattice. On the basis of the results discussed in section 3.4, we can assume that the stabilization of t-ZrO_2 at a lower temperature is associated with the presence of oxygen vacancies. Incorporation of Cu^+ or Cu^{2+} ions into the ZrO_2 network compensates for the negative charge of vacancies and further contributes to the stabilization of the tetragonal ZrO_2 phase. Our theoretical calculations, taking into account the contributions of the different lattice planes in monoclinic and tetragonal ZrO_2 polymorphs, showed that oxygen vacancies are formed easily on the (111) facet, which is favored in a tetragonal ZrO_2 phase at temperatures below 550 K, which is also in the area of high activity Cu/ZrO_2 catalysts. Cu cations located near the oxygen vacancies act as the electron acceptor, i.e., Lewis acid centers and OH groups associated with copper as the Brønsted ones. In contrast, metallic copper dispersed on the ZrO_2 surface produces atomic hydrogen as a result of dissociation of H_2 molecules.[1,3] The fact that the methanol formation rate depends on the concentration of acid centers containing copper cations indicates that dissociation of hydrogen must be fast and hydrogenation of one of the transition complexes, leading to methanol, is the controlling step of the reaction rate. This is consistent with the generally accepted opinion on the mechanism of this reaction, which indicates the hydrogenation of the surface formate as the slowest step.[1−3]

■ ASSOCIATED CONTENT

Supporting Information

Additional figures and tables. This material is available free of charge via the Internet at http://pubs.acs.org.

■ AUTHOR INFORMATION

Corresponding Author

*E-mail: ncgrabow@cyf-kr.edu.pl. Tel.: + 48 12 63 95 161.

Notes

The authors declare no competing financial interest.

■ ACKNOWLEDGMENTS

This work was supported by OPUS project no. 2012/05/B/ST4/00071 founded by the National Science Centre of Poland and Polish-French Cooperation Groupement De Recherche International (GDRI CNRS-PAN) "Catalysis for polluting emissions after treatment and production of renewable energies."

■ REFERENCES

(1) Kiennemann, A.; Hindermann, J. P. *Surf. Sci. Catal. Stud.* **1988**, *35*, 181−255.
(2) Hansen, J. B. In *Handbook of Heterogenous Catalysis*; Ertl, G., Knozinger, H., Weykamp, J., Eds.; Wiley-VCH: Weinheim, Germany, 1997; Vol. *4*, p 1.
(3) Skrzypek, J.; Słoczyński, J.; Ledakowicz, L. *Methanol Synthesis*; Polish Scientific Publishers (PWN): Warszawa, Poland, 1994.
(4) Halmann, M. L. Greenhouse Gas Carbon Dioxide Mitigation. *Science and Technology*; Process Sciences Group: Upton, NY, 1998.
(5) Haggin, J. *Chem. Eng. News* **1994**, *72*, 28−36.
(6) Hirano, M.; Akano, T.; Imai, T.; Kuroda, K. *Stud. Surf. Sci. Catal.* **1998**, *114*, 545−549.
(7) Breen, J. P.; Ross, J. R. H. *Catal. Today* **1999**, *51*, 521−533.
(8) Velu, S.; Suzuki, K.; Okazaki, M.; Kapoor, M. P.; Osaki, T.; Ohashi, F. *J. Catal.* **2000**, *194*, 373−384.
(9) de Wild, P. J.; Verhaak, M. J. F. M. *Catal. Today* **2000**, *60*, 3−10.
(10) Köppel, R. A.; Baiker, A.; Wokaum, A. *Appl. Catal., A* **1992**, *84*, 77−102.
(11) Amenomiya, Y. *Appl. Catal.* **1987**, *30*, 57−68.
(12) Bartey, G. J. J.; Burch, R. *Appl. Catal.* **1988**, *43*, 141−153.
(13) Nitta, Y.; Fujimatsu, T.; Okamoto, Y.; Imanaka, T. *Catal. Lett.* **1993**, *17*, 157−165.
(14) Fröhlich, C.; Köppel, R. A.; Baiker, A.; Kilo, M.; Wokaun, A. *Appl. Catal., A* **1993**, *106*, 275−293.
(15) Nitta, Y.; Suwata, O.; Ikeda, Y.; Okamoto, Y.; Imanaka, T. *Catal. Lett.* **1994**, *26*, 345−354.
(16) Sahibzada, M.; Chadwig, D.; Metcalfe, I. S. *Catal. Today* **1996**, *29*, 367−372.
(17) Kilo, M.; Weigel, J.; Baiker, A.; Wokaun, A.; Köppel, R. A.; Stoekli, A.; Baiker, A. *J. Mol. Catal. A: Chem.* **1997**, *126*, 169−184.
(18) Ma, Y.; Sun, Q.; Wu, D.; Fan, W.-H.; Zhan, Y.-L.; Deng, J.-F. *Appl. Catal., A* **1998**, *171*, 45−55.
(19) Joo, O.-S.; Jung, K.-D.; Moon, I.; Rozovskii, A. Y.; Lin, G. I.; Han, S.-H.; Uhm, S.-J. *Ind. Eng. Chem. Res.* **1999**, *38*, 1808−1812.
(20) Wambach, J.; Baiker, A.; Wokaun, A. *Phys. Chem. Chem. Phys.* **1999**, *1*, 5071−5080.
(21) Ortelli, E. E.; Wambach, J.; Wokaun, A. *Appl. Catal., A* **2001**, *216*, 227−241.
(22) Chinchen, G. C.; Denny, P. J.; Jennings, J. R.; Spencer, M. S.; Waugh, K. C. *Appl. Catal.* **1988**, *36*, 1−65.
(23) Saito, M.; Fujitani, T.; Takeuchi, M.; Watanabe, T. *Appl. Catal., A* **1996**, *138*, 311−318.
(24) Słoczyński, J.; Grabowski, R.; Olszewski, P.; Kozłowska, A.; Stoch, J.; Lachowska, M.; Skrzypek, J. *Appl. Catal., A* **2006**, *310*, 127−137.
(25) Baiker, A.; Kilo, M.; Maciejewski, M.; Manzi, S.; Wokaun, A. *Stud. Surf. Sci. Catal.* **1993**, *75*, 1257−1272.
(26) Ruh, R.; Rocket, T. J. *J. Am. Ceram. Soc.* **1970**, *53*, 360.
(27) Koppel, R.; Stocker, C.; Baiker, A. *J. Catal.* **1988**, *179*, 515−527.
(28) Ma, Z.-Y.; Yang, C.; Wie, W.; Li, W.-H.; Sun, Y.-H. *J. Mol. Catal. A: Chem.* **2005**, *231*, 75−81.
(29) Wang, L.-C.; Liu, Q.; Chen, M.; Liu, Y.-M.; Cao, Y.; Hey-Yong; Fan, K.-N. *J. Phys. Chem. C* **2007**, *111*, 16549−16557.
(30) Jung, K. T.; Bell, A. T. *Catal. Lett.* **2002**, *80*, 63−68.
(31) Rhodes, M. D.; Bell, A. T. *J. Catal.* **2005**, *233*, 198−209.
(32) Yamaguchi, T. *Catal. Today* **1994**, *20*, 199−217.
(33) Morterra, C.; Cerrato, G.; Signoretto, M. *Catal. Lett.* **1996**, *41*, 101−109.
(34) Morterra, C.; Cerrato, G.; Bolis, V.; Di Ciero, S.; Signoretto, M. *J. Chem. Soc., Faraday Trans.* **1997**, *93*, 1179−1184.
(35) Morterra, C.; Cerrato, G.; Di Ciero, S. *Appl. Surf. Sci.* **1998**, *126*, 107−128.
(36) Tanabe, K. *Mater. Chem. Phys.* **1985**, *13*, 347.
(37) Arena, F.; Italiano, G.; Barbera, K.; Bordiga, S.; Bonura, G.; Spadaro, L.; Frusteri, F. *Appl. Catal., A* **2008**, *350*, 16−21.
(38) Liu, X. M.; Lu, G. Q.; Yan, Z. F. *Appl. Catal., A* **2005**, *279*, 241−245.
(39) Reddy, B. M.; Thrimurthulu, G.; Katta, L.; Yamada, Y.; Park, S.-E. *J. Phys. Chem. C* **2009**, *113*, 15882−15890.
(40) Pokrovski, K.; Jung, K. T.; Bell, A. T. *Langmuir* **2001**, *17*, 4297−4303.
(41) Grabowski, R.; Słoczyński, J.; Śliwa, M.; Mucha, D.; Socha, R. P. *ACS Catal.* **2011**, *1*, 266−278.
(42) Piskorz, W.; Gryboś, J.; Zasada, F.; Cristol, S.; Paul, J.-F.; Adamski, A.; Sojka, Z. *J. Phys. Chem. C* **2011**, *115* (49), 24274−24286.
(43) Piskorz, W.; Gryboś, J.; Zasada, F.; Zapała, P.; Cristol, S.; Paul, J.-F.; Sojka, Z. *J. Phys. Chem. C* **2012**, *116* (36), 19307−19320.
(44) Pimentel, H. R. X.; Aguiar, D. L. M.; San Gil, R. A. S.; Souza, E. F.; Ferreira, A. R.; Leitão, A. A.; Alencastro, R. B.; Menezes, S. M. C.; Chiaro, S. S. X. *Chem. Phys. Lett.* **2013**, *555*, 96−100.
(45) Syzgantseva, O. A.; Calatayud, M.; Minot, C. *J. Phys. Chem. C* **2012**, *116*, 6636−6644.

(46) Gionco, C.; Paganini, M. C.; Giamello, E.; Burgess, R.; Di Valentin, C.; Pacchioni, G. *Chem. Mater.* **2013**, *25*, 2243−2253.
(47) Jomard, G.; Petit, T.; Pasturel, A. *Phys. Rev. B* **1999**, *59*, 4044−4052.
(48) Ceron, M. L.; Herrera, B.; Araya, P.; Gracia, F.; Toro-Labbe, A. *J. Mol. Model.* **2013**, *19*, 2885−91.
(49) Herrera, B.; Gracia, F.; Araya, P.; Toro-Labbe, A. *J. Mol. Model.* **2009**, *15*, 405−410.
(50) Grau-Crespo, R.; Hernandez, N. C.; Sanz, J. F.; de Leeuw, N. H. *J. Phys. Chem. C* **2007**, *111*, 10448−10454.
(51) Tang, Q.-L.; Hong, Q.-J.; Liu, Z.-P. *J. Catal.* **2009**, *263*, 114−122.
(52) Hong, Q.-J.; Liu, Z.-P. *Surf. Sci.* **2010**, *604*, 1869−1876.
(53) Tang, Q.-L.; Liu, Z.-P. *J. Phys. Chem. C* **2010**, *114*, 8423−8430.
(54) Jung, K. *J. Catal.* **2000**, *193*, 207−223.
(55) Cheary, R. W.; Coelho, A. A. *J. Appl. Crystallogr.* **1992**, *25*, 109−121.
(56) Tougaard, S. *Surf. Interface Anal.* **1993**, *21*, 165−176.
(57) Kresse, G.; Hafner, J. *Phys. Rev. B* **1994**, *49*, 14251−14251.
(58) Kresse, G.; Furthmuller, J. *Comput. Mater. Sci.* **1996**, *6*, 15−50.
(59) Perdew, J. P.; Chevary, J. A.; Vosko, S. H.; Jackson, K. A.; Pederson, M. R.; Singh, D. J.; Fiolhais, C. *Phys. Rev. B* **1992**, *46*, 6671−6688.
(60) Perdew, J. P.; Wang, Y. *Phys. Rev. B* **1992**, *45*, 13244−13249.
(61) Bloechl, P. E. *Phys. Rev. B* **1994**, *50*, 17953−17979.
(62) Kresse, G.; Joubert, D. *Phys. Rev. B* **1999**, *59*, 1758−1775.
(63) Zhao, Y.; Tao, K.; Wan, H. L. *Catal. Commun.* **2004**, *5*, 249−252.
(64) Moulder, J. F.; Stickle, W. F.; Sobol, P. E.; Bomben, K. *Handbook of X-ray Photoelectron Spectroscopy*, 2nd ed.; Perkin-Elmer Corporation (Physical Electronics): Waltham, MA, 1992.
(65) Electron Spectroscopy Database. www.lasurface.com.
(66) NIST X-ray Photoelectron Spectroscopy Database. http://srdata.nist.gov/xps/.
(67) Espinos, J. P.; Morales, A.; Barranco, A.; Caballero, A.; Holdago, J. P.; Gonzalez-Elipe, A. R. *J. Phys. Chem. B* **2002**, *106*, 6921−6929.
(68) Janas, J.; Gurgul, J.; Socha, R. P.; Dźwigaj, S. *Appl. Catal., B* **2009**, *91*, 217−224.
(69) Dźwigaj, S.; Janas, J.; Gurgul, J.; Socha, R. P.; Shishido, T.; Che, M. *Appl. Catal., B* **2009**, *85*, 131−138.
(70) Moretti, G. *J. Electron Spectrosc. Relat. Phenom.* **1995**, *76*, 365−370.
(71) Cui, X.; Takahashi, K.; Otsuki, T.; Iwai, H.; Egawa, C. *Surf. Sci. Nanotechnol.* **2009**, *7*, 898−903.
(72) Amano, F.; Suzuki, S.; Yamanoto, T.; Tanaka, T. *Appl. Catal. B: Environ.* **2006**, *64*, 282−289.
(73) Si, Z.; Weng, D.; Wu, X.; Jiang, Y.; Wang, B. *Catal. Sci. Technol.* **2011**, *1*, 453−461.
(74) Yu, Q.; Yao, X.; Zhang, H.; Gao, F.; Donga, L. *Appl. Catal., A* **2012**, *423*−*424*, 42−51.
(75) Shukla, S.; Seal, S. *Int. Mater. Rev.* **2005**, *50*, 45−64.
(76) Collins, D. E.; Bowman, K. J. *J. Mater. Res.* **1998**, *13*, 1230−1237.
(77) Osendi, M. I.; Moya, J. S.; Serna, C. J.; Soria, J. *J. Am. Ceram. Soc.* **1985**, *68*, 135−139.
(78) Jana, S.; Biswas, P. K. *Mater. Lett.* **1997**, *30*, 53−58.
(79) Bokhimi, X.; Morales, A.; Novaro, O.; Lopez, T.; Gomez, R.; Xiao, T. D.; Strut, P. R. *Nanostruct. Mater.* **1999**, *12*, 593−596.
(80) Norman, C. J.; Goulding, P. A.; McAlpine, I. *Catal. Today* **1994**, *20*, 313−322.
(81) Dwividi, A.; Cormack, A. N. *Philos. Mag. A* **1990**, *61*, 1−1.
(82) Morinaga, M.; Cohen, J. B.; Faber, J. J. *Acta Crystallogr., Sect. A* **1979**, *35*, 789−795.
(83) Stefanovich, E. V.; Shluger, A. L. *Phys. Rev. B* **1994**, *49*, 11560−11571.
(84) Joyner, R. W. *Catal. Lett.* **1990**, *6*, 151−156.
(85) Burch, R.; Golunski, S. E.; Spencer, M. S. *J. Chem. Soc. Faraday Trans.* **1990**, *86*, 2683−2689.
(86) Robinson, W. R. A. M.; Mol, J. C. *Appl. Catal.* **1990**, *63*, 165−179.